Nondestructive and Destructive Testing of Decommissioned Reinforced Concrete Slab Highway Bridge and Associated Analytical Studies

A. E. AKTAN, M. ZWICK, R. MILLER, AND B. SHAHROOZ

Recently there have been many examples of undesirable bridge performance under service loads and scour and after floods and earthquakes. There is also evidence that, according to present inspection and rating procedures, a large number of bridges may be deemed structurally deficient without justification. Many reinforced concrete (RC) slab bridges are now being replaced without taking full advantage of their inherent capacities because of a lack of understanding and knowledge of the effects of deterioration and aging on these bridges. To establish procedures to allow for the full utilization of RC slab bridge capacity, a 38-year-old sample was loaded to failure. The bridge, which was decommissioned because of its age and deteriorated state, endured the equivalent loading of 22 rating trucks before failure.

A legislatively mandated program to inventory, inspect, and improve the nation's bridges was initiated in 1977 after the collapse of the Silver Bridge over the Ohio River at Point Pleasant, W.Va. (*1*). This program has not been able to eliminate bridge collapses and failures completely: over only a 5-year window from 1977 through 1981, 14 cases of bridge collapse and an additional 19 cases of bridge failure short of collapse under service loads were documented (*2*). More recently, the vulnerability of bridges against natural hazards has been realized in the well-publicized collapses of the Schoharie Creek and Hatachie River bridges caused by scour (*3*) and the collapse of segments of the Nimitz freeway and the Bay Bridge in 1989 because of the Loma Prieta earthquake (*4*). Therefore, a more effective means of inspection and diagnosis is needed to evaluate bridge condition and vulnerability against collapse as a result of both traffic and natural hazards.

Certain bridge types, such as reinforced concrete (RC) slab bridges with sound piers and abutments, are inherently more resistant to collapse than others. Not a single RC slab bridge collapse was reported among the 33 cases studied by Hadipriono (*2*). An NCHRP review of field tests also has indicated that redundant bridges may have far greater strength than may be anticipated by the current rating methods (*5*). Other studies confirm this view (*6*). Many of these bridges have been, or are being, decommissioned without fully utilizing their available capacities. The financial implications can be staggering if one considers that the national bridge inventory as of 1987 listed 98,777 RC slab and T-beam bridges, of which 15,519 had an SR of less than 50, and 57,331 had an SR between 50 and 80. By recognizing and using all of the inherent capacities of these bridges, highway funds may be prioritized more effectively.

Department of Civil and Environmental Engineering, University of Cincinnati, Mail Location 71, Cincinnati, Ohio 45221.

OBJECTIVES OF RESEARCH

The first goal of this research is a rigorous study of the technical aspects of inspection, rating, maintenance, and decommissioning of RC slab bridges. The second goal is to assess the state of the art in some of the experimental and analytical tools needed for more effective infrastructure preservation. These included a modal test–based quantitative nondestructive evaluation (NDE) technique that has been developed by University of Cincinnati (UC) researchers for Ohio Department of Transportation (ODOT)/FHWA (*7*).

In this study researchers explore whether the modal test–based NDE technique can accurately diagnose the condition of a concrete bridge deck from over an asphalt overlay, and whether the technique would reveal if a bridge has been overloaded. Further objectives in the area of NDE include exploring the feasibility of using truck-load tests as an effective NDE procedure and calibrating the currently used visual rating procedures for identifying distress in slab bridges.

The analytical tools explored included linearized identification of three-dimensional (3D) finite element models for bridge rating and 3D nonlinear finite element analysis (NLFEA) of complete, aged bridges that may have properties affected by damage and deterioration.

TEST SPECIMEN

Description of Test Specimen

The test specimen (Figure 1) is a three-span, RC skewed slab bridge that was constructed in 1953. The piers are set on footings placed on the bedrock, whereas the abutments are placed on steel piles driven to the bedrock. The piers and abutments are all skewed at a 30-degree angle (Figure 1).

Material Properties

Design drawings indicate Class C concrete, whereas no reference was made to the reinforcing steel grade. Core samples

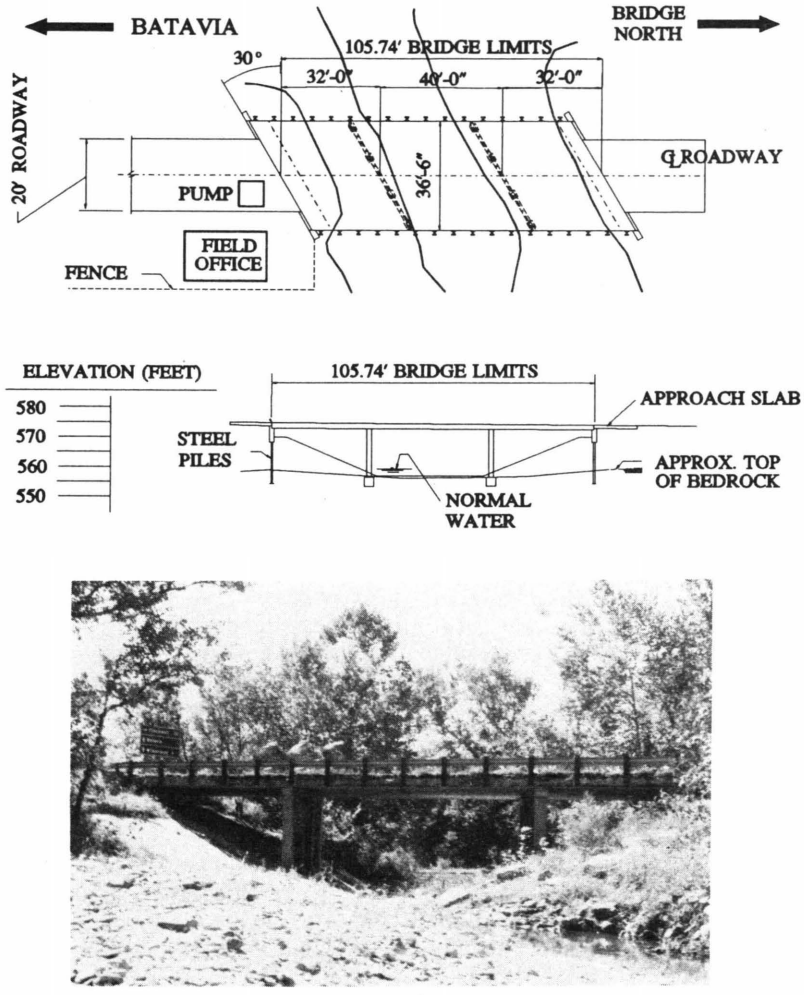

FIGURE 1 Description of test bridge: *top*, site plan; *middle*, site elevation; *bottom*, photograph.

4 in. in diameter through the asphalt overlay and the concrete deck were taken to study the material properties and their variation.

Concrete coring revealed that concrete in the shoulder regions was severely deteriorated. It was not possible to obtain sound cores from the shoulders since the concrete under the asphalt would crumble during coring, which jammed the coring bit. Throughout the driving lanes, full-depth, solid cores could be obtained.

Bridge Condition with Asphalt Overlay

Data for the initial damage surveys could not be collected from the top surface because of the presence of the asphalt overlay. An extensive effort was made toward searching for damage through the overlay by use of NDE techniques, because an overlay is common, especially over older bridge decks. These studies are described in the NDE section of the paper.

Although the bottom of the bridge did not exhibit any signs of extensive deterioration, the exposed sides of the bridge slab were heavily deteriorated. This damage was attributed to run-off mixed with salt used in deicing the bridge during winter months. Other than the heavily deteriorated sides, the survey revealed little other damage that was mostly limited to some light spalling and cracking on the bottom of the slab.

Bridge Condition After Removal of Asphalt Overlay

When the asphalt overlay was removed, the shoulder regions were found to be in an extremely deteriorated state, having completely lost the cover over a large number of bars. The concrete in the traffic lanes appeared reasonably solid. Extensive study and petrographic analyses of the concrete samples indicated that the primary agent in the deterioration was D-cracking of the porous coarse aggregate, which may have initiated during the freeze-thaw cycles of the first winter. The D-cracking left pathways in the concrete through which water and salt could pass. This cracking led to the secondary deterioration mechanism of alkali-silica reaction between some of the aggregates and the cement paste. The overlay was identified as a further facilitator of the deterioration by trap-

ping water between the overlay and concrete deck for long periods. After the cover concrete deteriorated, some of the reinforcing bars rusted, whereas others in the vicinity were observed to be in excellent shape.

The D-cracking near the top rebars opened up pathways for the water to enter and freeze, which induced spalling of the top layer of concrete. This primary deterioration mechanism is attributed to poor selection of materials and poorly implemented concrete construction. The deterioration was not triggered by corrosion of the reinforcing steel. Therefore, the deterioration of the bridge, within a short life span of only 38 years, could not have been avoided only by utilizing epoxy-coated rebars or cathodic protection. Instead, a possible deficiency with concrete material design specifications and the use of asphalt overlay are indicated.

NDE AND SUMMARY OF PRELIMINARY FINDINGS

Two methods of NDE were explored. The first is based on modal testing by impact and structural-identification developed at UC (*7*). The second procedure is based on monitoring bridge responses under static truck loads. Both of these procedures were performed on the bridge before removal of the asphalt overlay; this allowed the researchers to determine the effectiveness of NDE in diagnosing hidden damage and quantifying its effects on the mechanical characteristics of the structure. Modal tests were repeated after various stages of loading and damage during the destructive test program to explore if the modal test–based NDE technique would recognize damage caused by overloading. A complete reporting and evaluation of these tests is forthcoming; meanwhile the preliminary results of NDE conducted above the overlay are presented.

Modal Test–Based NDE Procedure and Preliminary Results

The NDE methodology is summarized in Figure 2. The methodology uses multireference modal testing to measure a sufficient number of mass-normalized mode shapes, frequencies, and damping coefficients that permit quantifying flexibility coefficients with respect to a fine discretization (*7*). Flexibility coefficients of even highly redundant structures may serve as a meaningful structural signature, as well as indexes sensitive to localized damage.

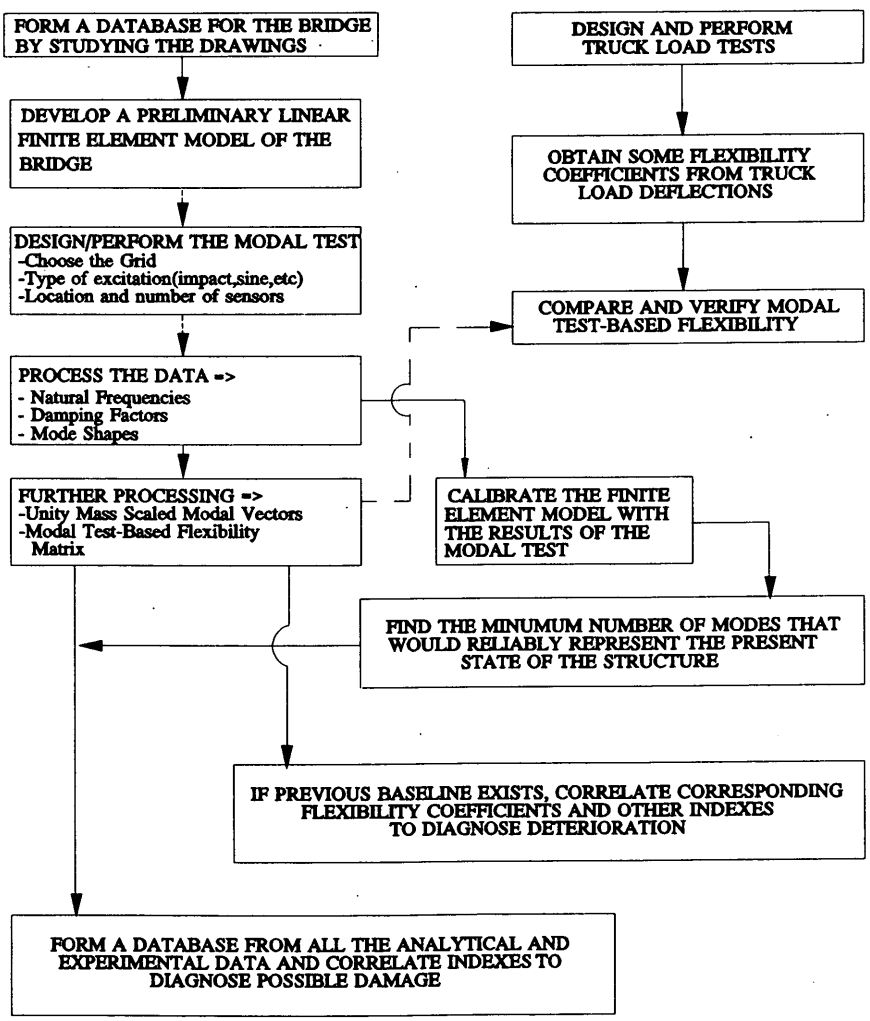

FIGURE 2 Summary of nondestructive evaluation.

Meanwhile, the measured dynamic characteristics are used to develop and numerically calibrate a linearized finite element (FE) model of the bridge in the absence of an experimental baseline. The calibrated FE model may serve as a basis for evaluating the dynamic test–based flexibility coefficients to diagnose damage. Research for establishing derivative indexes from flexibility to diagnose the influence of various forms of damage and deterioration of the capacities of a slab bridge is in progress. Naturally, if a reference flexibility is available from previous tests of the same bridge or tests of another benchmark bridge, damage diagnosis is facilitated.

Since the stress level arising from the modal test is typically much smaller than the stress level under truck traffic, a truck load test may help to validate the dynamic test–based flexibility. Truck load tests of typical slab or beam-slab bridges are generally impractical because measuring small displacements in the field is a difficult problem. Local strain measurement is not revealing, and in general it is possible to measure only a few displacements under truck loads. As a result, truck load tests do not lead to a finely discretized flexibility, as may be obtained from modal testing but serve to validate the reliability of results obtained from modal testing as well as a proof test if several multiples of legal loads may be safely applied.

Figure 3 compares some of the mode shapes and frequencies obtained from modal testing of the test bridge and the cor-

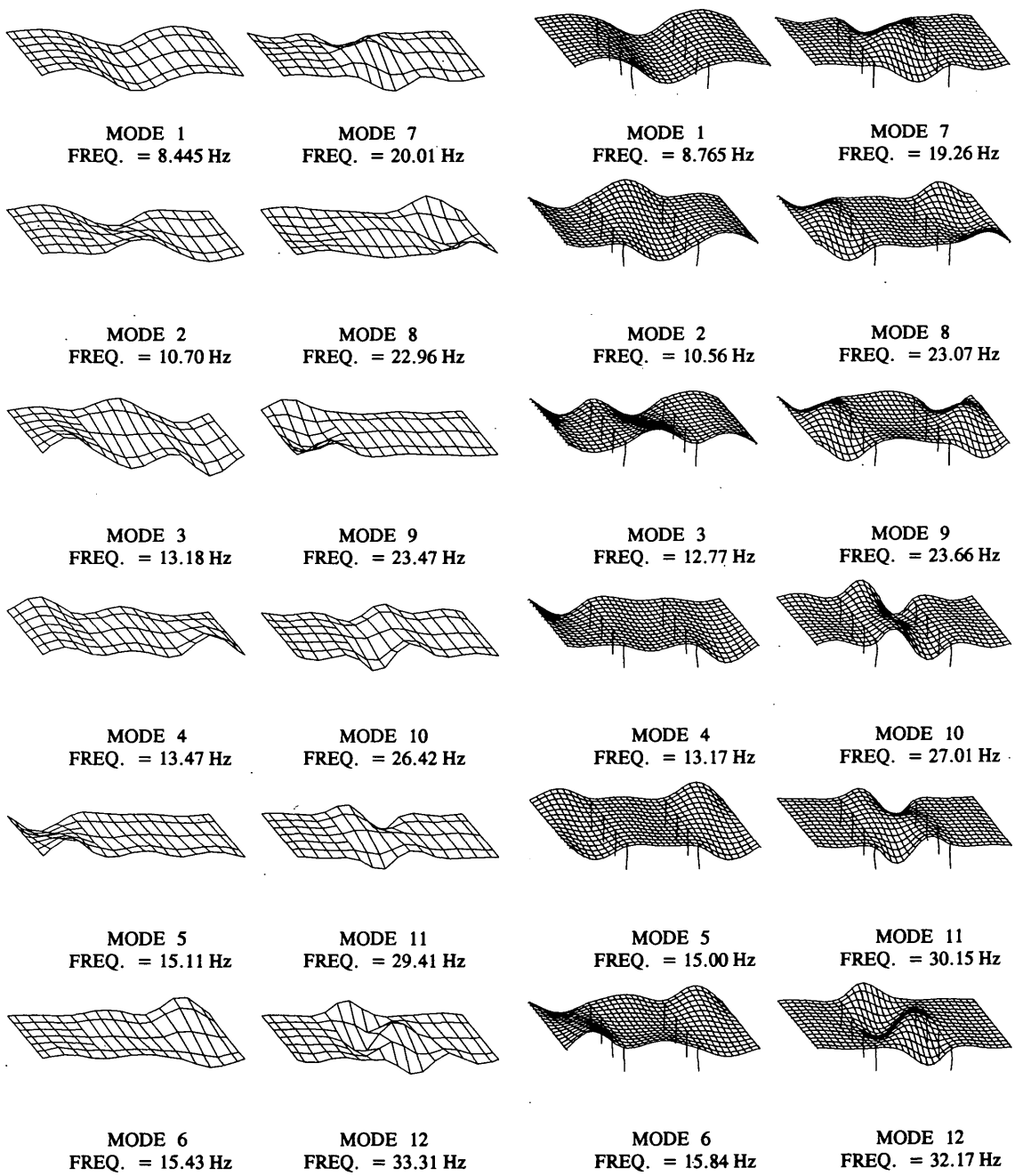

FIGURE 3 Comparison of experimental (*left*) and analytical (*right*) mode shapes.

responding dynamic characteristics of a calibrated FE model. Figure 4 compares some of the dynamic test–based flexibility coefficients with the corresponding coefficients of the calibrated analytical model. The coefficients correspond to bridge deflections along the transverse lines labeled D and I on the modal test grid shown in Figure 4, as a unit load is respectively placed at the midpoint of Lines D and I. The correlations reveal that the bridge is considerably more flexible than the "rational" analytical model along both Lines D and I. The difference between analytical and experimental deflections increases especially toward the east shoulder. These observations reveal that the structural properties of the slab are affected considerably by damage, particularly along the east shoulder. Research is in progress to extrapolate from the influence of damage on flexibility to the influence of damage on strength capacity.

Results of Truck Load Tests

Truck load tests were used to verify the flexibility from the modal test. Three single-axle dump trucks loaded with gravel were used. The tire weights were measured with portable scales, whereas the bridge deflections were measured at 21 points with sufficiently sensitive and specially calibrated and mounted electronic transducers. Bridge deflections measured along Line D under one and three trucks are compared with the corresponding deflections predicted from the calibrated analytical model and modal test–based flexibility in Figure 5. There are magnitude differences in deflections measured under truck loads and those predicted from the modal test-based flexibility, although the deflection patterns are similar. The differences are attributed to the difference in stress level at the impact and truck load tests in conjunction with non-

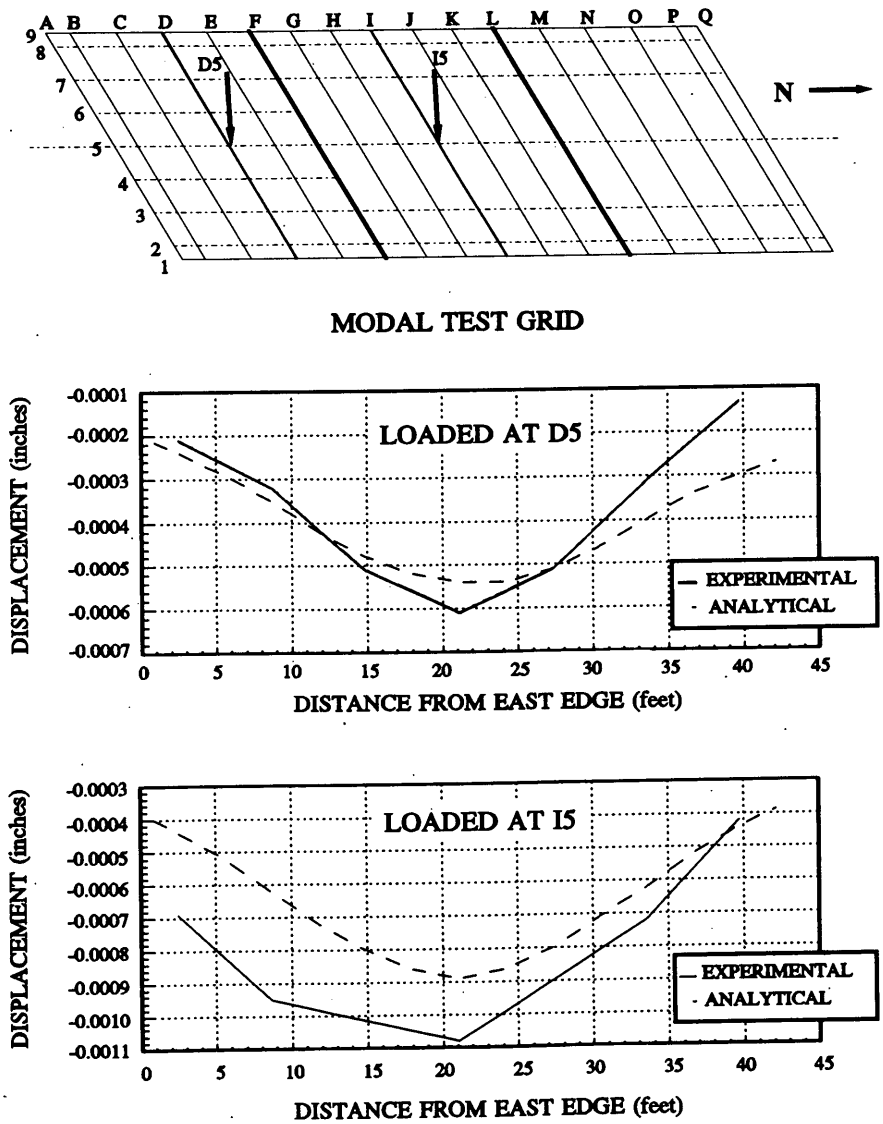

FIGURE 4 Comparison of experimental and analytical flexibility.

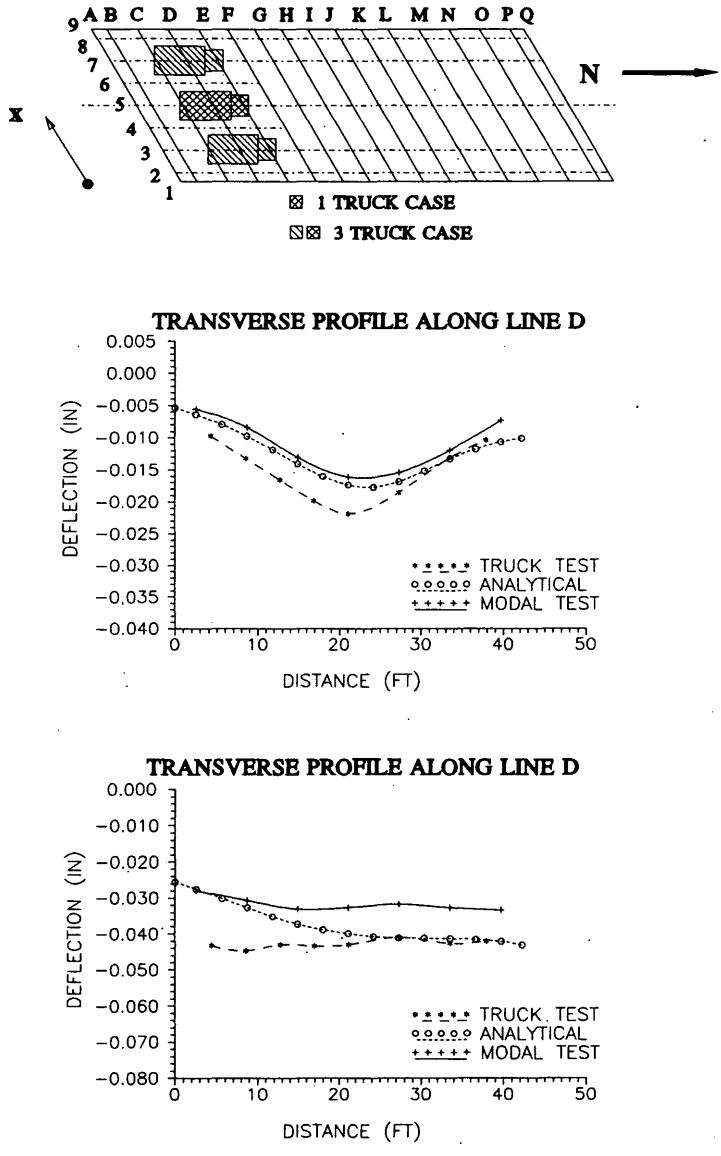

FIGURE 5 Comparison of truck load test flexibility: *top*, truck load configurations; *middle*, one-truck case; *bottom*, three-truck case.

linearity. Although the "rational" analytical model indicates that the flexibility of the east shoulder should be considerably less than the flexibility along the west shoulder because of skew, in reality both the truck load measurements and modal test–based flexibility are contrary, indicating that there should be relatively higher damage along the east shoulder.

PREDICTIVE ANALYSES

Predictive analyses were performed to design the loading setup and to establish the loading program. Another objective was to evaluate the state of the art in NLFEA for predicting behavior of reinforced concrete bridges. Linear finite element analyses and yield line analyses were also performed to support NLFEA.

Researchers from the Delft Technological University (the Netherlands) collaborated with UC researchers at this step of the research. The analyses performed by Delft were helpful in assessing the state of the art since the software (DIANA) developed by the Delft group, as well as the NLFEA expertise represented by this group, is considered some of the best in the world (*8*).

Figure 6 (*top*) shows the geometric characteristics of the analytical model used by UC for the NLFEA. The initial boundary stiffness at the abutments of this model was established through structural identification, incorporating the dynamic characteristics of the bridge measured by modal testing. Although concrete cracking, concrete plasticity, and yielding

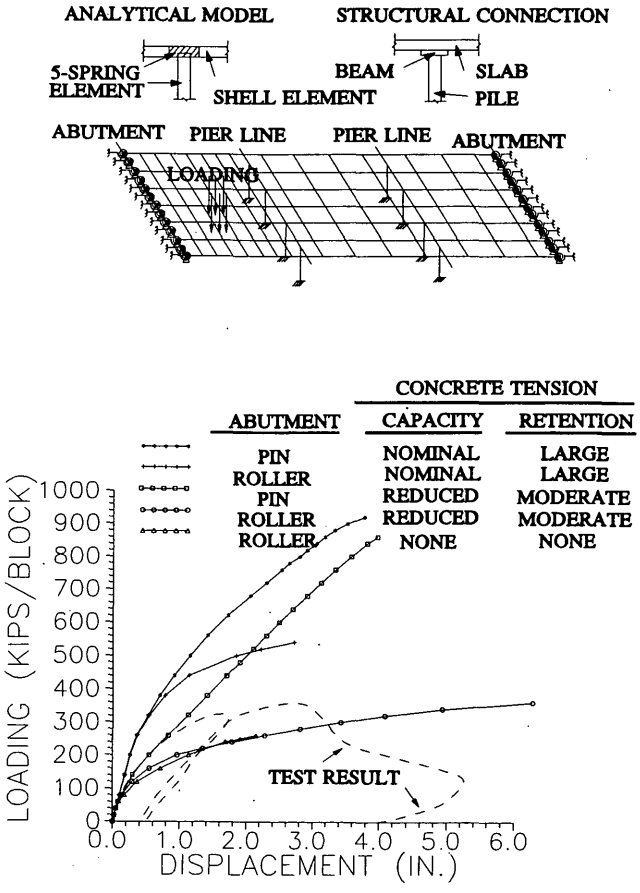

FIGURE 6 NLFEA model (*top*) and results of NLFEA analyses (*bottom*).

of reinforcing bars were accounted for during the NLFEA, the boundary conditions were not. However, subsequent to the tests, it became apparent that the boundary conditions at the abutment comprised the most critical parameter.

Figure 6 (*bottom*) shows some of the predicted global responses of the bridge conducted by UC compared with the corresponding measured response during the test. Analytical responses demonstrate the significance of parameters that define the boundary conditions at the abutment and the stress-strain response of concrete under uniaxial tension. These parameters are associated with the greatest uncertainty in analyzing the bridge, although the modal test results and standard material test responses were available.

The sensitivity of analytical responses to the described boundary and material parameters indicates that it is not yet possible to rely on NLFEA to predict available capacities and failure modes of slab bridges. This analytical tool may serve to understand the critical parameters for optimizing the design of new bridges or the upgrade of existing ones.

DESIGN OF LOADING AND DATA ACQUISITION

Loading Position

A decision was made to simulate a one-lane, one-trailer loading during the test, although a multilane loading of the bridge would have been more critical for rating. One-lane loading permitted the observation of more complex modes of slab-bridge behavior, and made it possible to extend the findings to estimate with reasonable reliability the bridge capacity under multilane loading. Figure 7 shows the position and manner of the loading applied to the bridge during the tests, along with the truck it is simulating. The load simulated the front tandem of a trailer as it is entering the bridge in the northbound lane. Analyses indicate the southbound lane of the loaded end span to be stiffer than the northbound lane, as discussed earlier, in relation to the truck load test responses (see Figure 7). However, NDE also revealed that the loss of stiffness caused by damage at the northbound lane and shoulder at this end span was more critical than at the southbound lane. Therefore, the decision was made for loading the southeast quadrant of the bridge to reveal the extent of the influence of damage and deterioration on bridge behavior.

The destructive test loading simulated loading of the bridge as envisioned in the rating process based on the *AASHTO Manual of Maintenance Inspection* (*9,10*), as opposed to the actual dynamic manner in which the traffic load is imposed on the bridge. The rationale behind loading the bridge statically is clear: it permits one to test the reliability of the rating process, especially as it applies to the computing of capacity and demand for RC slab bridges.

Design of Loading and Loading Control Systems

Predictive analyses indicated that the upper bound of the bridge load capacity may be as high as 1,400 kips (about 40 rating trucks) for the loading position that was selected. The loading system was designed for this upper bound. It is not feasible to apply this level of load without hydraulic cylinders. Moreover, applying the load to the bridge while simulating tire loads and without creating local crushing was a challenge. An even greater challenge was the manner in which reaction could be developed in applying this type of load.

On the basis of lengthy research and feasibility analyses, it was decided to use rock anchors to develop the reaction and to pour two concrete blocks directly on the bridge to simulate the footprints of a tandem trailer (Figure 7). The blocks were designed to accommodate the four hydraulic cylinders (actuators), each with 350-kip capacity and 12-in. stroke. Double-acting actuators were acquired with a 4-in.-diameter hole through their length to accommodate eight-strand rock anchor cables.

To fabricate the loading setup, four cores were drilled in the bridge deck to allow for the drilling of the rock anchors and to allow the cables from the rock anchors to pass through the bridge deck. The rock-anchors were then installed and the concrete loading blocks were fabricated. The cables passed through the bridge deck, the concrete load blocks, and each actuator. The strands were then locked by wedges at the top of the actuator, so that as the actuator extended, the rock-anchors provided the reaction needed to load the bridge (Figure 7).

A state-of-the-art servocontrolled electrohydraulic loading system that consisted of a pump, the four actuators, two servovalves, a two-channel digital servocontroller, pressure feedbacks for load control, and stroke feedbacks for displacement

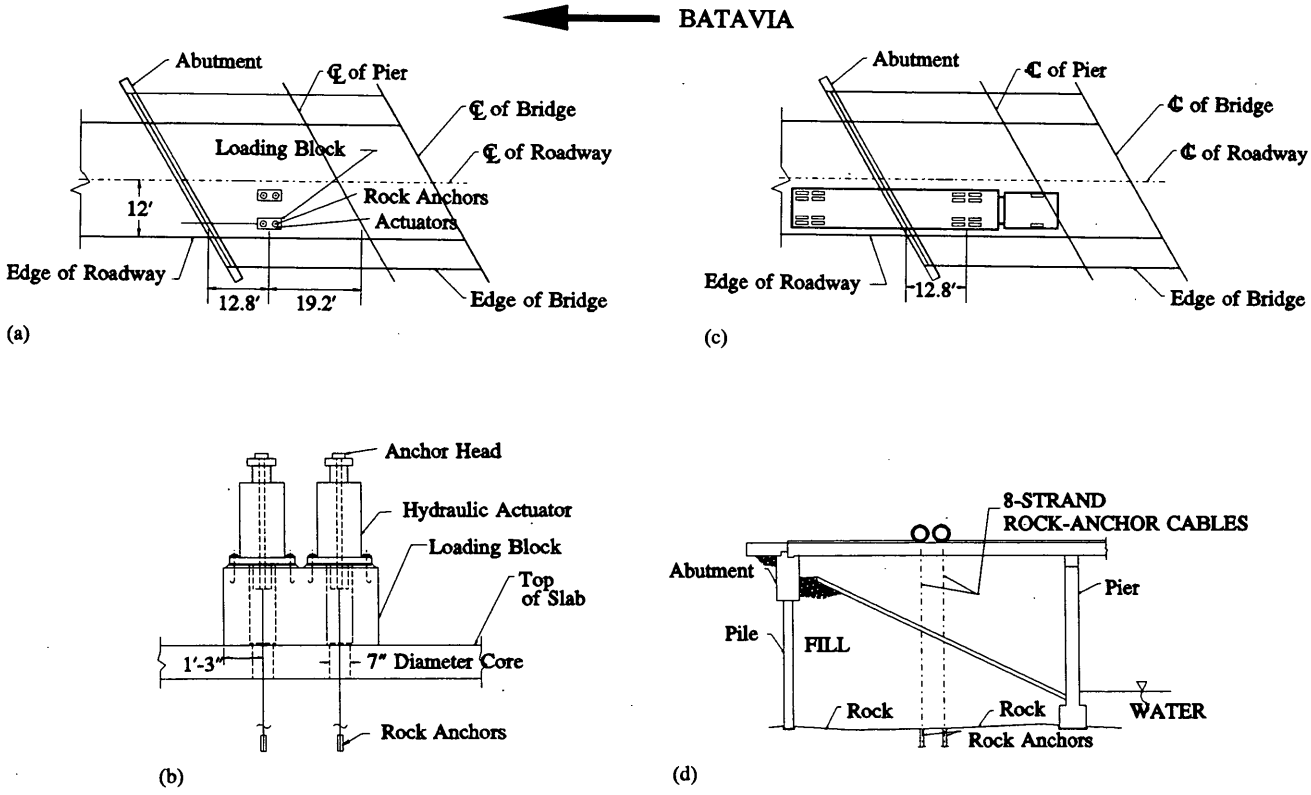

FIGURE 7 Plan view (*a*) and elevation view (*b*) of loading system; plan view (*c*) and elevation view (*d*) of simulated loading.

control was developed for loading. Together with the servocontrol system, real-time digital plotting was used for instantaneous feedback of actuator loads, strokes, and critical specimen responses. This real-time system provided the information needed to make decisions for commanding the servocontrol system. The test control and data acquisition systems were located and controlled at a field office adjacent to the bridge.

Instrumentation and Data Acquisition Systems

A principal objective of the experiment was to evaluate the state of the art in NLFEA. Therefore, extensive global and local instrumentation that would permit comprehensive correlations between analytically predicted (and subsequently simulated) and measured responses of the bridge was required. Such instrumentation was designed on the basis of the results of preliminary analyses conducted by UC and Delft; more than 160 transducers were placed on the bridge. These electronic transducers measured the forces and strokes of the four actuators, vertical and lateral displacements of the slab, slab rotations at the abutment and pier, concrete distortions, and steel strains through the critical regions of the slab.

Global instrumentation consisted of wire potentiometers used to measure the vertical displacements of the bridge deck, and DC-linear variable differential transducers (DC-LVDTs) used to measure the horizontal movements of the bridge deck. For the local instrumentation, DC-LVDTs and clip gauges were used to measure concrete distortions, and pier and abutment rotations. Foil strain gauges were placed on several rebars. All the wire potentiometers, DC-LVDTs, and clip gauges were calibrated in the laboratory through their expected operating spans. The transducer readings were recorded by data acquisition systems supplied by UC and WJE.

Design of Loading Program

Design of the loading program was aided by the upper-bound load-displacement response predicted by the NLFEA, and adjustments were made as the actual responses of the bridge were observed. First the bridge was rated based on the 1989 AASHTO guide specifications (*1*) to establish a rating factor corresponding to an impact factor of unity and to the single-lane load simulation developed for the test. The calibrated 3D finite element model discussed earlier in reference to NDE was used to estimate the demands. This procedure indicated a rating factor of 4.95. Therefore, a test load corresponding to the weight of five rating trucks was considered to signify the upper limit of the serviceability limit state for the bridge. Throughout the test, loading was applied in increments of rating trucks, where one rating truck corresponded to a total of 32 kips (one tandem weight) on the two loading blocks.

Figure 8 shows the load versus vertical displacement response measured next to the loading block near the shoulder (Point C3 shown in the inset). The first stage of the test was composed of numerous loading and unloading cycles that corresponded to shakedown at the serviceability limit state. These cycles also permitted debugging the test control, loading, and

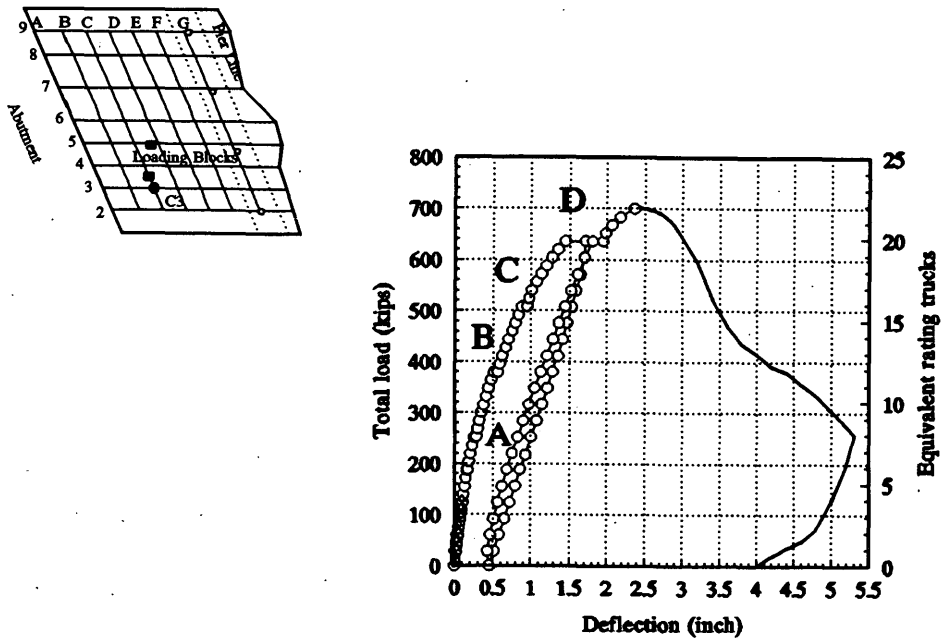

FIGURE 8 Load displacement response at Point C3.

operation of the data acquisition systems. The service-level load cycles were followed by a large inelastic excursion that revealed the damageability limit state characteristics of the bridge and left a permanent vertical deformation of about 0.5 in. after unloading. The final leg of loading led to the failure of the bridge and left a permanent deformation exceeding 4 in. (Figure 8).

Preliminary Results

The limit states indicated by the load versus load-point deflection response of the bridge are marked on Figure 8, corresponding to 7, 13, 17, and 21 truckloads. Each limit state corresponds to a change of stiffness at the load point. These limit states were attributed to progressive cracking of the slab and were also strongly influenced by the slab rotations at the abutment.

To monitor rebar strains at the critical regions, 19 strain gauges were installed on the top and bottom bridge reinforcement in the vicinity of the loading points and near the abutment and pierline. It is significant that none of these gauges indicated yielding before the load level reached 20 truckloads. At a load of 20 truckloads, several of the gauges in the vicinity of the loading blocks indicated initiation of yielding. It follows that the nonlinearity observed in the global load-deflection response in Figure 8 up to a level of 20 truckloads is not caused by yielding.

Figure 9 shows the three points along the abutment where slab rotations relative to the abutment were measured as well as the corresponding load-versus-rotation envelopes. At many limit states marked on the global load-deflection response in Figure 8, the rotational stiffness provided to the slab by the abutment at locations corresponding to Gridlines 3 and 6 experienced a marked change. It follows that changes in the boundary conditions of the slab at the abutment, with increasing load level, played a significant role in the behavior of the bridge up to its failure.

Behavior at Failure Limit State

The damageability limit state behavior (between 7 and 21 truckloads, Figure 8) of the bridge did not reveal any alarming signs of distress although 20 truckloads corresponded to over four times the load the bridge was rated for. Even under sustained 20 truckloads, experienced ODOT bridge engineers did not have any reservations about inspecting the underside of the loaded bridge. Although there was extensive cracking, no distinct yield lines had emerged.

When the load was increased to the equivalent of 22 rating trucks, the bridge failed in a brittle manner. The topside view of the failure plane is shown in Figure 10. The failure was apparently triggered by a diagonal tension failure at the edge of the pier-slab interface in the damaged shoulder region. The failure front then progressed along the pierline until, at about the midpoint of the bridge, it followed a circular path arching back toward the abutment. This failure front followed top-bar cutoff points along most of its circular path. The servo-control system maintained a considerable portion of the failure load until it was turned off, as reflected in the postfailure response in Figure 8. In spite of the brittle nature of the failure, a considerable postfailure strength reserve is implicated. Dowel action of the bottom longitudinal bars that were continuous from the abutment and through the pier was particularly effective in preventing the total collapse of the end span and providing the postfailure strength.

Although a more detailed study of the failure mechanism is in progress, it is relevant that the average shear stress within the failure plane was less than $1.0\sqrt{f'_c}$. A photograph of the topside view of failure is shown in Figure 10 (*bottom*).

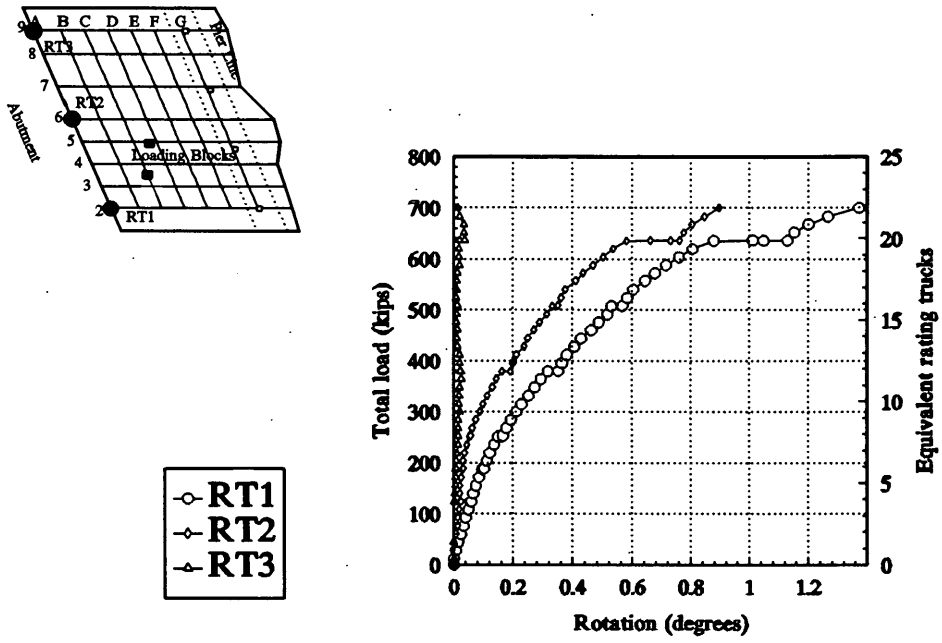

FIGURE 9 Rotational response at abutment.

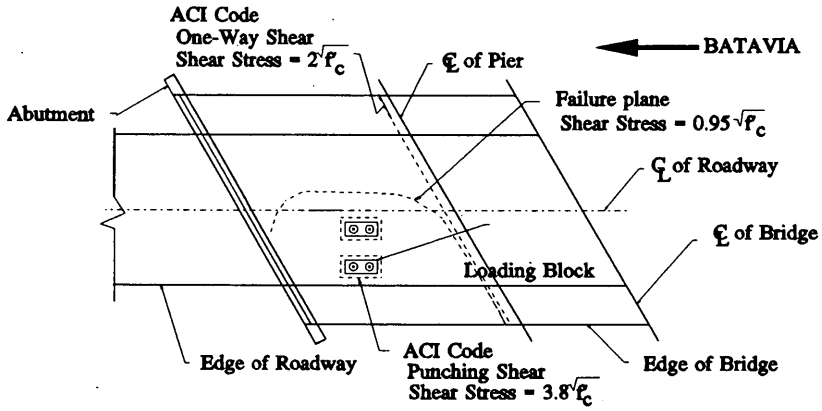

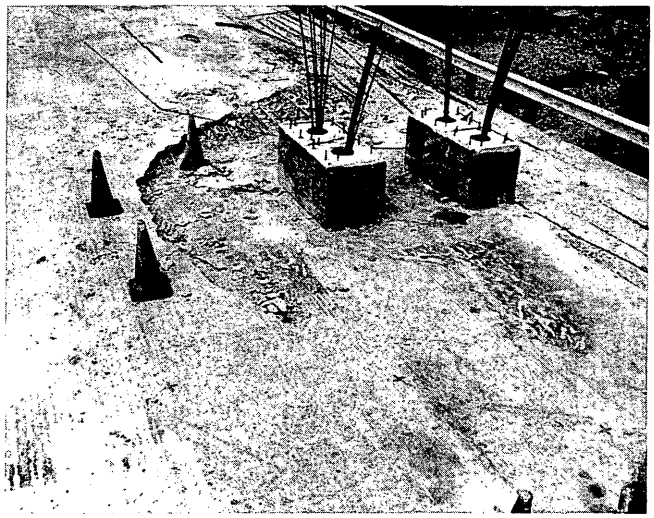

FIGURE 10 Description of failure plane: *top*, plan view; *bottom*, photograph.

PRELIMINARY CONCLUSIONS

The modal test-based NDE procedure holds great promise in diagnosing concrete deterioration and damage hidden under asphalt overlay. The procedure also leads to a calibrated linearized FE model of the bridge that is the key for reliably rating a bridge per the 1989 AASHTO specifications. The capability of the modal test–based NDE procedure to diagnose overload-related damage is promising, as will be reported subsequently.

The truck load tests may serve as an NDE tool as well although instrumentation is difficult and the results do not lead to the comprehensive information that is revealed by a rigorous modal test. The stress level at a truck load test is much higher than the stress level during the impact-modal test. However, considering that the service level stiffness of the bridge did not decrease appreciably until the bridge was loaded by more than five trucks, the differences in the stress levels of the impact test and the truck load tests do not seem very important in bridge diagnostics unless the conditions warrant a proof test.

Bridge engineers should start recognizing the inherent capacities in RC slab bridges that have sound abutments and piers. Even with the extensive deterioration of shoulder concrete, the test bridge safely carried more than 20 rating trucks, a load exceeding four times the bridge rating based on a calibrated FE model. It follows that bridge rating and decommissioning based on only visual inspection may greatly underestimate the actual capacity of slab bridges. Considering that the average replacement cost of a two-lane, three-span, approximately 100-ft-long slab bridge is in the order of $250,000, the financial implications of using these bridges over longer life spans with some maintenance is significant.

The mechanics of the deterioration involved environmental attack directly on the concrete, indicating that measures such as using epoxy-coated rebars or cathodic protection would not avoid all kinds of bridge deterioration. Instead, concrete materials and additives should be specified to eliminate possible alkali attacks or other chemical reactions that may cause deterioration. Concrete should be designed for maximum resistance against cracking and surface deterioration. The mechanical and microchemical characteristics of coarse aggregate are most important parameters and should be adequately specified.

The inability to predict bounds of nonlinear responses of the bridge within a narrow band even by using state-of-the-art software and expertise point to the difficulty in analytically estimating RC bridge capacity. In particular, the failure mode could not be predicted, and it is doubtful that it is possible to properly simulate the failure that was observed in an analytical model. The much simpler limit analyses that were carried out could reveal the possible bounds of the strength capacity with as much error or accuracy as the NLFEA; however, they could not have been used for estimating stiffness characteristics. The assumed concrete tension response and modeling the boundary conditions of the slab at the abutment were found as the most critical parameters influencing significantly the predicted structural response.

Obviously, predicting bridge capacity by NLFEA within a narrow band is not possible since response is very sensitive to a considerable number of parameters that cannot be established with confidence even if the boundary conditions of the bridge are established at the service limit states and the materials are sampled and tested. The sensitivity of RC slab bridges to parameters such as the tension response of concrete is unlike RC beams or bare frames, the strength of which are less sensitive to similar parameters.

The mode of failure of the skew slab was not anticipated as it was not previously experienced in laboratory tests of slabs. In fact, there are no code provisions that would guide a designer to check against this type of shear failure in slab design. The failure initiated as diagonal tension failure at the interface of the slab and pier and was apparently triggered because of the damage to slab concrete at the edge of the pier.

The average shear stress within the failure plane was less than $1.0\sqrt{f'_c}$, which is much less than what is generally expected as the shear capacity of concrete, even in one-way flexural shear. Because of the delamination in the shoulder concrete, no shear resistance may have been provided by the concrete along a certain percentage of the failure plane. This may explain the low level of average shear stress at failure within the failure plane. Obviously, the capacities and failure modes of aged constructed facilities may be profoundly influenced by any existing damage and deterioration. Therefore, an attempt to evaluate the capacities of an aged constructed facility without understanding and incorporating its existing conditions will not be realistic. The existing conditions of a constructed facility cannot be established without nondestructive experimentation coupled with sampling and testing of the materials.

ACKNOWLEDGMENTS

The authors wish to acknowledge the project sponsors, FHWA/ODOT and the National Science Foundation (NSF). The authors acknowledge K. Chong, of NSF, and W. Edwards, V. Dalal, D. Hanhilammi, R. Eltzroth, and W. Fair, of ODOT, as well as many ODOT personnel who provided crucial support and advice throughout the research. At the University of Cincinnati, the authors wish to acknowledge graduate students Ho, Hrinko, Heckenmueller, and Toksoy; research engineer C. Young; and technician D. Strunk for their valuable contributions. M. Carlier of the Manta Corporation designed and operated the electrohydraulic servocontrolled loading system. Invaluable consultation and collaboration were provided by R. Iding and D. Meinheit and D. Heidbrink from Wiss, Janney, Elstner, Associates of Chicago. The authors further recognize the collaboration of the Delft Technological University of the Netherlands. Goettle Corporation provided invaluable support by installing the rock anchors, and the Sheffer Corporation provided the loading actuators at a subsidized cost.

REFERENCES

1. R. A. Imbsen, W. D. Liu, R. A. Schamber, and R. V. Nutt. *NCHRP Report 292: Strength Evaluation of Existing Reinforced Concrete Bridges*. TRB, National Research Council, Washington, D.C., 1987.

2. F. C. Hadipriono. Analysis of Events in Recent Structural Failures. *Journal of Structural Engineering*, ASCE, Vol. 111, No. 7, July 1985, pp. 1468–1481.
3. F. Huber. Update: Bridge Scour. *Civil Engineering*, ASCE, New York, N.Y., Sept. 1991.
4. Loma Prieta Earthquake Reconnaissance Report. In *Earthquake Spectra*, Supplement to Vol. 6, Earthquake Engineering Research Institute, May 1990.
5. E. G. Burdette and D. W. Goodpasture. *NCHRP Report 306: Correlation of Bridge Load Capacity Estimates With Test Data*. TRB, National Research Council, Washington, D.C., 1988.
6. B. Bakht and L. G. Jaeger. Bridge Testing—A Surprise Every Time. *Journal of Structural Engineering*, ASCE, Vol. 116, No. 5, pp. 1370–1383.
7. A. E. Aktan and M. Raghavendrachar. *Nondestructive Testing and Identification For Bridge Rating: Pilot Project*. Report FHWA/ODOT-90/005, May 1990.
8. J. G. M. Van Mier. Examples of Non-Linear Analysis of Reinforced Concrete Structures with DIANA. *HERON*, Vol. 32, No. 3, 1987.
9. *Manual of Maintenance Inspection*. AASHTO, Washington, D.C., 1983.
10. *Manual of Maintenance Inspection*. AASHTO, Washington, D.C., 1989.

The conclusions presented are the opinions of the authors only.

Publication of this paper sponsored by Committee on Dynamics and Field Testing of Bridges.